Research Article | DOI:10.5281/zenodo.8007891
www.jnanosam.com

NANOSAM
Journal of NanoScience in Advanced Materials

Tailoring Magnetic Properties of Fe-CoNi Core-Shell Nanostructures by using Two-Step Electrodeposition Method

Saroj Parajuli[1,2#] and Muhammad Irfan[3]

Core-shell nanogeometries are class of nonstructural materials have been lively in the area of research for their sizable applications. Iron (Fe) electrodeposited inside Cobalt-Nickle (CoNi) alloy nanotubes (NTs) were fabricated using a two-step dc electrodeposition method within the nanopores of anodized aluminum oxide (AAO) template. Fe-CoNi core-shell nano architectures were crystalline in nature. The X-ray diffraction and electron microscopy confirmed the presence of face cubic centre (fcc) in both Fe and CoNi at core and shell region. Curling magnetization reversal mechanism has been explained by angular dependence of coercivity (H_c). At Low temperature H_c of NTs and core-shell nanostructures follow the thermal activation model. Temperature dependence of H_c of both nanoconfiguration ensue the 3/2 power law for the field dependence of energy barrier. Deviation between FC and ZFC decline progressively with rise in temperature.

1. Introduction

Since the 20th century, nanotechnology has been used intensively in the fields of engineering and science, which are very active and important research areas. One-dimensional (I-D) magnetic nanomaterials (MNM), such as nanotubes (NTs), nanowires (NWs), core-shell nanorods (CSN), nanocrystals, etc. have low dimensionality and high surface–to–volume ratio as promising building blocks as the future of optoelectronic devices, solar cells, biotechnology, nanomedicine, photovoltaic, optical detection, medical therapy, etc. [1-5] that enhance a range of physical properties. I-D MNM recurrently display high chemical reactivity in NWs oxidation and contaminations lowering the act for nanodevices. It also serves as a protective cover on a given nanogeometries that keep the work durability. Core-shell structures (CSS) are the perfect choice for forthcoming generations for numerous applications.

To date, there are various ways of fabrication of core-shell nanocylinders [6-8] such as sol-gel method [9, 10] hydrothermal [11], solvothermal [12], chemical vapor deposition (CVD) [13], pulse lager deposition [14], molecular beam epitaxy [15]. I-D MNMs with core and shell from substances having particular structure according to the projected applications. However, these processes are expensive and time-consuming. Due to this reason, we have employed two step electrochemical deposition of metals on anodic aluminum oxide (AAO) template for synthesis of core-shell nanowires (CSNWs) as a more economical process. A series of nanostructures of metals or alloys, semiconductors, polymers and many more materials finished within nanochannels of AAO templates [16, 17]. I-D core-shell nanostructures (CSNS) which could form additional effects in fundamental physics have been reported earlier.

There was only little research interest on the fabrication of core-shell nanogeometry by using two-step electrodeposition way [18-21]. A simple method which can produce nanogeometries over a large area being easily scaled up to a commercial level at very low cost. In first step electrodeposition, the shell grows inside the AAO templates nanopores with an exact potential. Here, CoNi allow NTs act as a shell. The fabrication of core materials followed the same electrodeposition methodology which was further electrodeposited inside the shell geometry. Since, Fe act as core substances. In this way, materials like Fe and CoNi NTs as core and shell can be electrodeposited separately and the thickness of each and every layer can also be accurately adjusted.

In current work, we have synthesis Fe-CoNi CSNS by using a simple AAO template-assisted two-

[1]Chinese Academy of Sciences, Institute of Physics, 100190, Beijing, China, [2]Tribhuvan University, Goldengate International College, 44621, Kathmandu, Nepal, [3]The Islamia University of Bahawalpur, Institute of Physics, 63100, Bahawalpur, Pakistan
#Corresponding author: mesaroj_999@hotmail.com

Keywords: Fe-CoNi Core-Shell NWs; Two-step Electrodeposition; Magnetization reversal mechanism; ZFC-FC curve.

Received: 19 April 2023 | Accepted: 29 May 2023 | Published online: 25 June 2023

step electrodeposition method to excel in the deposition of one material. The production of CSNWs with iron (Fe) and Cobalt Nickle (CoNi) alloy NTS were studied core and shell respectively. The morphological structures, composition, magnetic properties of the hybrid CSNS were carried out at room temperature and at lower temperatures confirm soft ferromagnetism. This is the detailed mechanism for Fe-CoNi magnetic CSS synthesis.

2. Results and Discussion

The prepared Fe-CoNi CSNWs morphology is studied by using field emission scanning electron microscopy(FE-SEM) as shown in Figs.1(a-b). The SEM images in Figs.1(a-b) show the highly ordered CoNi alloy NTs and core-shell nanostructures of Fe-CoNi. The synthesis CSNS with CoNi alloy NTs and Fe NWs as shell and core respectively with clear TEM image as shown in Fig.1(c). The energy dispersive X-ray spectroscopy (EDS) analysis the composition of magnetic CSNS that is in Fig.1(d) which displays the various elements as Fe, Co and Ni along with other elements like gold (Au), carbon (C), oxygen (O) and Aluminum (Al) in the CSNS. Here, Au is due to coating at the back side which served as the working electrode during the electrodeposition, carbon coated grid used for SEM, oxygen vacancies due to air and AAO templates made up Al.

CoNi alloy NTs is present with atomic ratio 50-50 percentage of each Co and Ni and so the XRD peak in Fig.2(a) matched with PDF card 04-004-8490. The CoNi alloy NTs XRD is highly crystalline in nature with face centered cubic (FCC) phase. It was seen that the broad peak due to alumina templates appeared around 38° this is exactly due to AAO template which is not perfectly etched. After second electrodeposition some peaks are presented as in the Fig.2(b). These addition peaks indicated that they are the mixture CoNi alloy NTs matched with Fe peaks. The reading of all these peaks has the excellent node with the standard peak's places for Co, Ni and Fe with FCC phase in Fe-CoNi CSNS.

The magnetic hysteresis loop has been recorded at room temperature (RT) under external magnetic field applied parallel and perpendicular to MNS axis. Figures 3(a, b) show the hysteresis loops of CoNi alloy NTs and CSNS follows the curling reversal mechanism [22, 23] due to the diameter thickness 't' of AAO. The coercivity is given by the relation,

$$H_c = \frac{A(A+1)}{\sqrt{A^2+2A+cos^2\theta}}\frac{M_S}{2} \quad (1)$$

For larger angle θ the magnetization reversal mechanism dominated by curling reversal mode. The angular dependence of coercivity curve for curling mode of magnetization reversal for both CoNi alloys NTs and Fe-CoNi CSNS from zero degree to 360 degrees are shown in Figs.3(c, d). H_c increases with the curling rotation mode gives the lowest and the highest H_C values for H parallel and perpendicular to the axis of nanostructures. The CoNi alloy NT's and Fe-CoNi core-shell nanoconfiguration coercivity is given in Table 1.

The H_c value increases as angle (θ) increases as in above equations fit for both the values. Temperature causes an active magnetization reversal in the magnetic NTs as well as core-shell nanoarchitecture.

Temperature causes an active magnetization reversal in both the CoNi alloy magnetic NTs and Fe-CoNi CSNS. The impact of temperature on the magnetic properties is essential to broaden objectionable effects. The low temperature spontaneous magnetization of magnetic materials due to Bloch law. In this report, the validity of Bloch law for temperature dependence of coercivity is determined for both CoNi alloy NTs and Fe-CoNi CSNWs. The Bloch law's mathematical expression is given as

$$H_c(T) = H_c(0)\left[1-\left(\frac{25k_BT}{E}\right)\right]^{1/m} \quad (2)$$

Here, $H_c(0)$ the switching field without thermal fluctuation, the height of barrier in the absence of external field E and k_B be the Boltzmann constant [24, 25]. The temperature dependence of H_c formula as, $H_c = \frac{H_c(T)}{H_c(0)} = H_c(0)[1-BT^n]$. Here, B is Bloch constant and n=1/m. According to Neel and Brown's thermal effect with an energy barrier is given by,

$$E = KV\left[1-\left(\frac{H}{H_0}\right)\right]^m \quad (3)$$

At temperature, T= 0K, the switching field and anisotropic energy are represented by H_c and KV, respectively.

Figures 4(a-b) are well-suited with equation (2) with the value of m equal to 1.5 reveals that H_c decrease as temperature increases, such a behavior of temperature verses coercivity (T vs H_c) are obtained in a series of loops measured at 5K to RT at 1 kOe for CoNi NTs and Fe-CoNi CSNS. In the current work, the rising of H_c with decreasing temperature expose magnetization reversal process being thermally activated. The fitting of overall data at every point in our both sample is nearly equal to 1.5.

Table 1. Coercieve fields of Fe-CoNi core-shell and CoNi shell in parallel and perpendicular directions.

Name	Parallel	Perpendicular
Core-Shell (Fe-CoNi)	271 Oe	401 Oe
Shell (CoNi)	290 Oe	482 Oe

NANOSAM
Journal of NanoScience in Advanced Materials

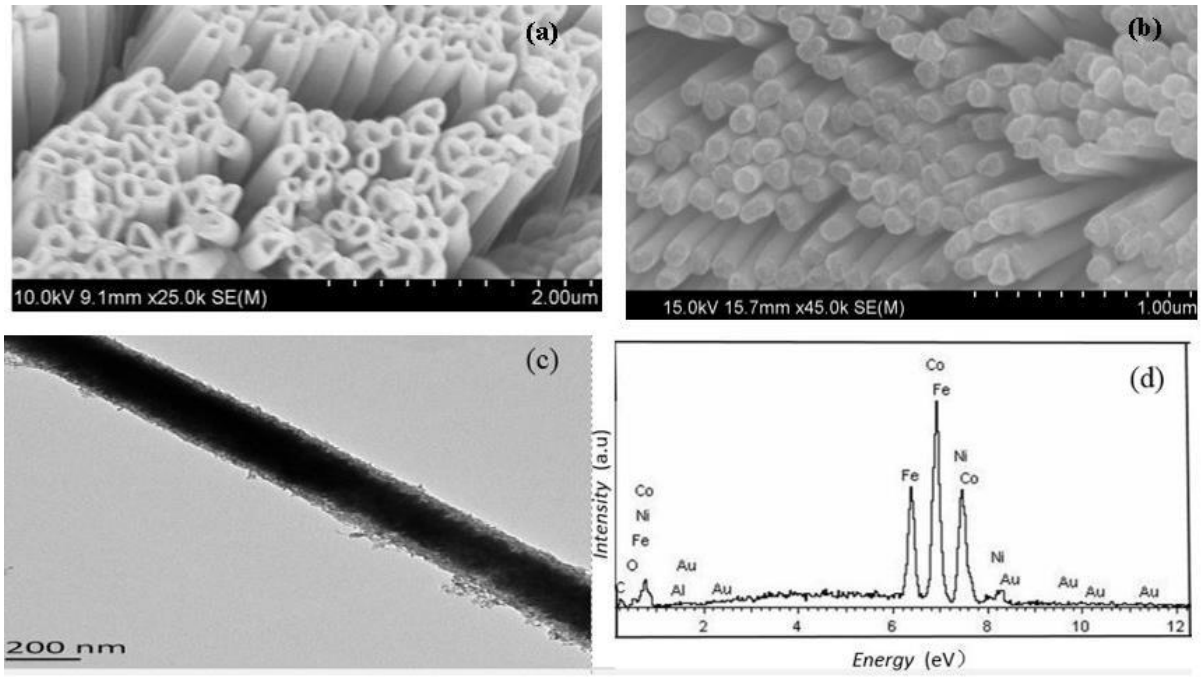

Figure 1. (a)SEM images of CoNi NTs, (b) SEM images of Fe-CoNi CSNWs,(c) TEM image of Fe-CoNi CSNWs and (d)EDX analysis.

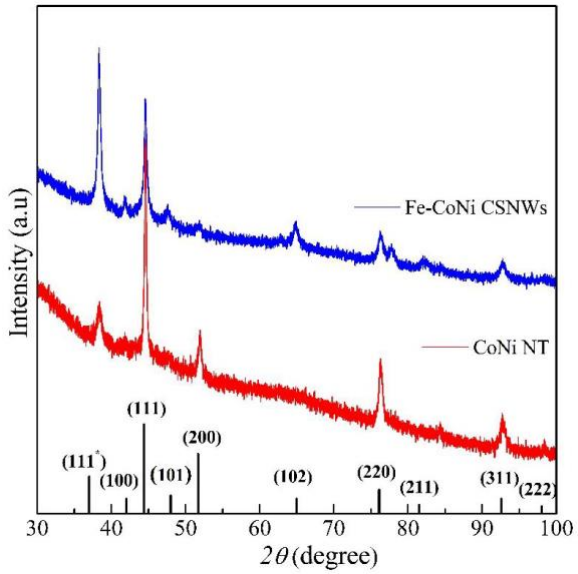

Figure 2. XRD images of CoNi NTs and XRD images of Fe-CoNi CSNWs.

Actually, 3/2 power law is the non-symmetric energy landscape. Now, the energy barrier per unit volume achieved from fitting the power law along with anisotropic energy of the sample can be calculated by using Eq.(3).

The temperature dependence of magnetization of both the nanogeometries after zero-field cooling (ZFC) and in field cooling (FC) were measured by sweeping temperature. Figures 5a-b show the ZFC-FC curves for CoNi NTs and Fe-CoNi CSNWs, respectively. The samples CoNi NTs and Fe-CoNi CSNS were cooled from RT to 5 K without any field in ZFC. At magnetic field intensity 1000 Oe and 300 K the samples were heated [24, 26, 27]. Same 1000 Oe magnetic field intensity is kept constant during cooling to 5 K in FC procedure. The deviation between FC and ZFC decline progressively with incline in temperature. FC and ZFC magnetization curves bifurcate from each other at temperature of irreversibility T_{irr}. Due to the large magnetic coercive field, large bifurcation in CoNi NTs and Fe-CoNi CSNS has been observed. The temperature of local maxima T_{max} on ZFC curves explained as average blocking temperature T_B and the difference between T_{irr} and T_{max} that follow to the wide distribution of T_B.

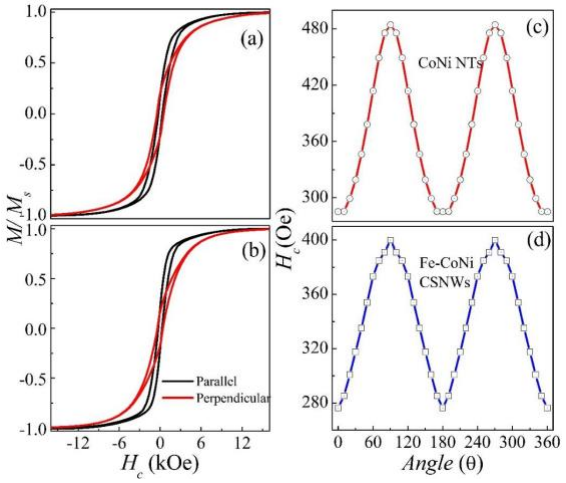

Figure 3. (a and b) MH images of CoNi NTs and Fe-CoNi CSNWs, (c and d) Angular dependence of Hc of CoNi NTs and Fe-CoNi CSNWs.

NANOSAM
Journal of NanoScience in Advanced Materials

Some physical characteristics are observed in the samples as a reversible trend are seen below T_B with $M_{ZFC} < M_{FC}$ given by the relation

$$M_{ZFC} = M_{FC}\left[\frac{H}{H_c+H}\right] \quad (4)$$

Both ZFC and FC magnetization decrease above T_B and Tc maximum value of ZFC can be calculated at $T_{max} < T_B$ [28]. Mathematical expression for T_B given as

$$T_B = \frac{K_m}{K}\left[\frac{V_m}{\ln T_m f_0}\right] \quad (5)$$

The experimental results are in good agreement with the given theoretical formulas.

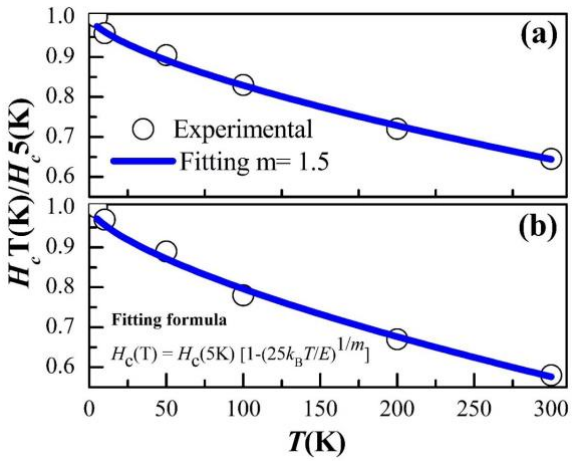

Figure 4. Normalized coercivity as a function of temperature for (a) CoNi NTs.and (b) Fe-CoNi CSNWs. The lines are fitting curves using Equation (2) when m=1.5.

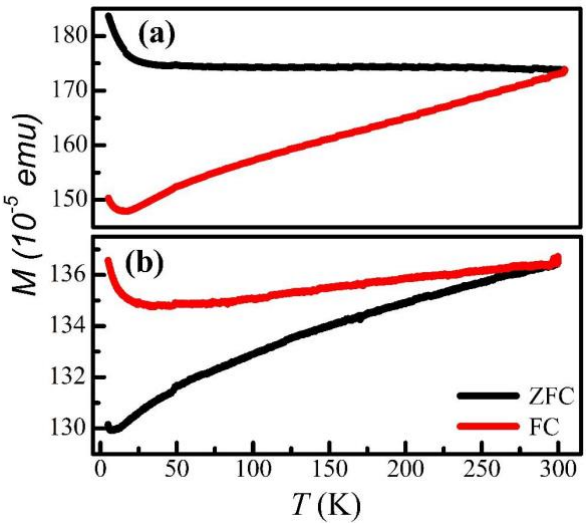

Figure 5. (a) ZFC-FC curves for CoNi NTs and (b) Fe-CoNi CSNWs.

3. Conclusion

In this study, Fe-CoNi CSNWs were fabricated by using two-step dc electrodeposition in the nanopores of AAO templates of thickness nearly equal to 200 nm. The XRD result of both CoNi NTs and Fe-CoNi CSNS were confirmed to be in FCC phase. The VSM result were reliant as the curling magnetization reversal mode for both CoNi NTs and Fe-CoNi nanostructures due to the larger diameter of AAO template. Both nanomagnetic geometries have significant anisotropy. H_c value of CSNS was lesser than NTs. The angular dependence of coercivity curve for curling mode of magnetization reversal for both CoNi alloys NTs and Fe-CoNi core-shell nanogeometry from 0 degree to 360 degree. At low temperature magnetic studied explain the HC of NTs and CSNS follows the thermal activation model. H_c were inclined with declining temperature modified Bloch law. The temperature dependence of H_c brought in the 3/2 power law for the field dependence of energy barrier for hysteresis. With rise in temperature the deviation between FC and ZFC declined progressively.

Method

The fabrication of Fe-CoNi CSNWs using high purity and uniform pore density AAO templates with an average pore diameter of 200 nm by a double electrodeposition process. On one side of the AAO templates a thin layer (10 nm) of gold (Au) was sputtered. The layer just covered the AAO between the nanopores leaving the cavity open, furnish as a working electrode. Electrodeposition was carried out in the three-electrode cell. Ag/AgCl act as the reference electrode, Pt foil as the counter electrode. While making CoNi NTs, a $CoSO_4.6H_2O$ and $NiSO_4.6H_2O$ (Sinopharm Chemical Reagent Co., Ltd, China with nearly 98% purity) was used as a precursor. The first electrodeposition was done for 1 hour at -1V reduction potential. In the final step, Fe NWs have grown in these CoNi NTs using $FeSO_4.7H_2O$ was also from Sinopharm Chemical Reagent Co., Ltd, China with nearly 98% purity. with boric acid (H_3BO_3) as electrolyte for 1 hour at -1.1V. Morphology of Fe-CoNi CSNS was explored with the use of Field Emission Scanning Electron Microscope (FE-SEM: Hitachi S-4800) and composition analysis done with energy dispersive X-ray spectroscopy (EDS) integrated with FE-SEM. Transmission Electron Microscope(TEM) diagnosed the core-shell nanostructures of the samples. The samples were structurally examined by the help of X-ray diffraction (XRD: RIGAKU-D/MAX-2400, CuKα, λ=0.154056nm). Vibrating Sample Magnetometer (VSM) was used to determine the magnetic properties of the samples. The field dependence of

the magnetization *M(H)* and temperature dependence magnetization *M(T)* of samples were studied with the help of Quantum Design Physical Property Measurement System (PPMS).

Acknowledgements

This work was supported by the National Key Research and Development Program of China [Grant No. 2017YFA0206200, 2016YFA0300802], the National Natural Science Foundation of China [NSFC, Grant No. 51831012,51761145110], and partially supported by the Strategic Priority Research Program (B) [Grant No. XDB33000000],the Key Research Program of Frontier Sciences (Grant No.QYZDJ-SSW-SLH016), and the International Partnership Program (No.112111KYSB20170090) of the Chinese Academy of Sciences (CAS), and Beijing Natural Science Foundation(Grant No. Z201100004220006).

Authors' contributions:

S.P.: Conceptualization, Formal analysis, Validation, Investigation, Writing and original draft. M. I.: Formal analysis.

Data Availability Statement

The data that support the findings of this study are available from the corresponding author upon reasonable request.

References

[1] Iijima, S. "Helical microtubules of graphitic carbon", Nature **354** (6348) 56-58 (1991).

[2] Bauer, U., Emori, S., and Beach, G.S.D. "Voltage-controlled domain wall traps in ferromagnetic nanowires", Nature nanotechnology **8** (6) 411-416 (2013).

[3] Wang, J. "Biomolecule-functionalized nanowires: from nanosensors to nanocarriers", Chemphyschem **10** (11) 1748-55 (2009).

[4] Park, S., Ko, H., Kim, S., and Lee, C. "Role of the Interfaces in Multiple Networked One-Dimensional Core–Shell Nanostructured Gas Sensors", ACS Applied Materials & Interfaces **6** (12) 9595-9600 (2014).

[5] Paravannoor, A., Ranjusha, R., Asha, A.M., Vani, R., Kalluri, S., Subramanian, K.R.V., Sivakumar, N., Kim, T.N., Nair, S.V., and Balakrishnan, A. "Chemical and structural stability of porous thin film NiO nanowire based electrodes for supercapacitors", Chemical Engineering Journal **220** 360-366 (2013).

[6] Kaydashev, V.E., Kaidashev, E.M., Peres, M., Monteiro, T., Correia, M.R., Sobolev, N.A., Alves, L.C., Franco, N., and Alves, E. "Structural and optical properties of Zn0.9Mn0.1O/ZnO core-shell nanowires designed by pulsed laser deposition", Journal of Applied Physics **106** (9) (2009).

[7] Ali, S.S., Li, W.J., Javed, K., Shi, D.W., Riaz, S., Liu, Y., Zhao, Y.G., Zhai, G.J., and Han, X.F. "Utilizing the anti-ferromagnetic functionality of a multiferroic shell to study exchange bias in hybrid core–shell nanostructures", Nanoscale **7** (32) 13398-13403 (2015).

[8] El-Toni, A.M., Habila, M.A., Labis, J.P., Alothman, Z.A., Alhoshan, M., Elzatahry, A.A., and Zhang, F. "Design, synthesis and applications of core–shell, hollow core, and nanorattle multifunctional nanostructures", Nanoscale **8** (5) 2510-2531 (2016).

[9] Irfan, M., Wang, C.J., Khan, U., Li, W.J., Zhang, X.M., Kong, W.J., Liu, P., Wan, C.H., Liu, Y.W., and Han, X.F. "Controllable synthesis of ferromagnetic–antiferromagnetic core–shell NWs with tunable magnetic properties", Nanoscale **9** (17) 5694-5700 (2017).

[10] Zhang, X.M., Li, W.J., Irfan, M., Parajuli, S., Wei, J.W., Yan, Z.R., Wang, X., Ahmad, N., Feng, J.F., Yu, G.Q., and Han, X.F. "Fabrication and characterization of YIG nanotubes", Journal of Magnetism and Magnetic Materials **482** 358-363 (2019).

[11] Chen, Y.-J., Xiao, G., Wang, T.-S., Ouyang, Q.-Y., Qi, L.-H., Ma, Y., Gao, P., Zhu, C.-L., Cao, M.-S., and Jin, H.-B. "Porous Fe3O4/Carbon Core/Shell Nanorods: Synthesis and Electromagnetic Properties", The Journal of Physical Chemistry C **115** (28) 13603-13608 (2011).

[12] Pal, B., Dhara, S., Giri, P.K., and Sarkar, D. "Room temperature ferromagnetism with high magnetic moment and optical properties of Co doped ZnO nanorods synthesized by a solvothermal route", Journal of Alloys and Compounds **615** 378-385 (2014).

[13] Chen, Y.-J., Gao, P., Wang, R.-X., Zhu, C.-L., Wang, L.-J., Cao, M.-S., and Jin, H.-B. "Porous Fe3O4/SnO2 Core/Shell Nanorods: Synthesis and Electromagnetic Properties", The Journal of Physical Chemistry C **113** (23) 10061-10064 (2009).

[14] Jie, J., Zhang, W., Bello, I., Lee, C.-S., and Lee, S.-T. "One-dimensional II–VI nanostructures: Synthesis, properties and optoelectronic applications", Nano Today **5** (4) 313-336 (2010).

[15] Rudolph, A., Soda, M., Kiessling, M., Wojtowicz, T., Schuh, D., Wegscheider, W., Zweck, J., Back, C., and Reiger, E. "Ferromagnetic GaAs/GaMnAs Core–Shell Nanowires Grown by Molecular Beam Epitaxy", Nano Letters **9** (11) 3860-3866 (2009).

[16] Al-Kaysi, R.O., Ghaddar, T.H., and Guirado, G. "Fabrication of One-Dimensional Organic Nanostructures Using Anodic Aluminum Oxide Templates", Journal of Nanomaterials **2009** 436375 (2009).

[17] Tian, Y.T., Meng, G.M., Wang, G.Z., Phillipp, F., Sun, S.H., and Zhang, L.D. "Step-shaped bismuth nanowires with metal–semiconductor junction characteristics", Nanotechnology **17** (4) 1041 (2006).

[18] Chen, J.Y., Ahmad, N., Shi, D.W., Zhou, W.P., and Han, X.F. "Synthesis and magnetic characterization of Co-NiO-Ni core-shell nanotube arrays", Journal of Applied Physics **110** (7) (2011).

[19] Narayanan, T.N., Shaijumon, M.M., Ajayan, P.M., and Anantharaman, M.R. "Synthesis of High Coercivity Core–Shell

Nanorods Based on Nickel and Cobalt and Their Magnetic Properties", Nanoscale Research Letters **5** (1) 164 (2009).

[20] Wang, J., Xiong, W., Huang, L., Li, Y., Zuo, Z., Hu, X., Wang, T., Xiao, J.Q., and Hu, J. "Electrochemical synthesis of core-shell Co-Ni nanorod arrays with facilely regulated magnetic properties", Physica B: Condensed Matter **567** 113-117 (2019).

[21] Chen, Y., Duan, J., Yao, H., Mo, D., Wang, T., Sun, Y., and Liu, J. "Preparation and magnetic properties of Cu-Ni core-shell nanowires in ion-track templates", Journal of Wuhan University of Technology-Mater. Sci. Ed. **30** (4) 665-669 (2015).

[22] Han, X.-F., Shamaila, S., Sharif, R., Chen, J.-Y., Liu, H.-R., and Liu, D.-P. "Structural and Magnetic Properties of Various Ferromagnetic Nanotubes", Advanced Materials **21** (45) 4619-4624 (2009).

[23] Zeng, H., Skomski, R., Menon, L., Liu, Y., Bandyopadhyay, S., and Sellmyer, D.J. "Structure and magnetic properties of ferromagnetic nanowires in self-assembled arrays", Physical Review B **65** (13) 134426 (2002).

[24] Hansen, M.F. and Mørup, S. "Estimation of blocking temperatures from ZFC/FC curves", Journal of Magnetism and Magnetic Materials **203** (1) 214-216 (1999).

[25] Sharif, R., Shamaila, S., Shaheen, F., Chen, J.Y., Khaleeq-ur-Rahman, M., and Hussain, K. "Bloch law for ferromagnetic nanotubes", Applied Physics Letters **102** (1) (2013).

[26] Bruvera, I.J., Mendoza Zélis, P., Pilar Calatayud, M., Goya, G.F., and Sánchez, F.H. "Determination of the blocking temperature of magnetic nanoparticles: The good, the bad, and the ugly", Journal of Applied Physics **118** (18) (2015).

[27] Livesey, K.L., Ruta, S., Anderson, N.R., Baldomir, D., Chantrell, R.W., and Serantes, D. "Beyond the blocking model to fit nanoparticle ZFC/FC magnetisation curves", Scientific Reports **8** (1) 11166 (2018).

[28] Concas, G., Congiu, F., Muscas, G., and Peddis, D. "Determination of Blocking Temperature in Magnetization and Mössbauer Time Scale: A Functional Form Approach", The Journal of Physical Chemistry C **121** (30) 16541-16548 (2017).